

Percolation-to-hopping crossover in conductor-insulator composites

G. Ambrosetti,^{1,*} I. Balberg,² and C. Grimaldi^{1,†}

¹*LPM, Ecole Polytechnique Fédérale de Lausanne, Station 17, CH-1015 Lausanne, Switzerland*

²*The Racah Institute of Physics, The Hebrew University, Jerusalem 91904, Israel*

Here, we show that the conductivity of conductor-insulator composites in which electrons can tunnel from each conducting particle to all others may display both percolation and tunneling (*i.e.*, hopping) regimes depending on few characteristics of the composite. Specifically, we find that the relevant parameters that give rise to one regime or the other are D/ξ (where D is the size of the conducting particles and ξ is the tunneling length) and the specific composite microstructure. For large values of D/ξ , percolation arises when the composite microstructure can be modeled as a regular lattice that is fractionally occupied by conducting particles, while the tunneling regime is always obtained for equilibrium distributions of conducting particles in a continuum insulating matrix. As D/ξ decreases the percolating behavior of the conductivity of lattice-like composites gradually crosses over to the tunneling-like regime characterizing particle dispersions in the continuum. For D/ξ values lower than $D/\xi \simeq 5$ the conductivity has tunneling-like behavior independent of the specific microstructure of the composite.

PACS numbers: 64.60.ah, 73.40.Gk, 72.80.Tm, 72.20.Fr

I. INTRODUCTION

The conductivity of a conductor-insulator composite material is characterized by a strong dependence on the volume fraction ϕ of the conducting phase present in the system, and is generally understood as a percolation phenomenon arising from the electrical connectivity between neighboring or adjacent conducting particles. Specifically, percolation theory considers the conducting particles as either electrically connected, with some finite inter-particle conductance, or disconnected.^{1,2} The introduction of this sharp cut-off implies then that below a specific fraction ϕ_c (the percolation threshold) the conductivity is zero because there is no sample-spanning network of connected particles, while for $\phi > \phi_c$ such network is formed and the conductivity increases as $\simeq (\phi - \phi_c)^t$, where t is a critical exponent.

It is easy to see that the notion of a sharp cut-off applies well to composites made of large (of the order of one micron or more) conducting particles, for which two particles can be considered electrically connected only if they essentially touch each other, it is less clear for the case in which the conducting particles have sizes limited to a few nanometers.³ In that situation even if the particles do not physically touch each other, their mean separation in the composite is such that electrons can still flow via tunneling processes from one particle to the other. The resulting tunneling conductance decays exponentially with the inter-particle distance over a characteristic tunneling length ξ which is of the order of a fraction to a few nanometers depending on the material properties. Since the tunneling decay does not imply any sharp cut-off, the basic assumption of percolation theory in describing composites made of nanometric conducting fillers is not justified a priori. In fact, it turns out that nanocomposites in the dielectric regime, for which the conducting particles do not touch each other, are better explained by inter-particle tunneling, with no imposed

sharp connectivity criterion, than by the classical percolation theory.^{4,5} The resulting conductivities of these systems follow therefore hopping-like (or tunneling-like) behaviors,⁶⁻⁹ with no critical percolation thresholds as a function of ϕ .

The possibility of having percolation-like or tunneling-like regimes depending on the size D of the conducting particles compared to the tunneling length ξ , as suggested above and in Ref.[3], does not appear to have been further elaborated in the literature, despite of its relevance to the understanding of transport properties in conductor-insulator composites. In the present paper we address this issue by considering a global tunneling network (GTN) model of conductor-insulator composites,⁵ where each conducting particle is connected to all others via tunneling processes. We show that this model permits to treat the percolation and the tunneling regimes on equal footing, and that one can switch from one regime to the other depending not only on D/ξ but, most notably, also on the specific distribution of the conducting phase in the composite. We illustrate this behavior by considering two idealized realizations of conductor-insulator composites: a lattice model, where conducting spherical particles of diameter D occupy randomly a fraction of the sites of a regular lattice, and a continuum model, where the conducting particles are dispersed with an equilibrium distribution in a continuous insulating medium. By using both the effective medium approximation (EMA) and Monte Carlo (MC) calculations, we find that the conductivity of the continuum model has a tunneling-like behavior independent of the value of D/ξ , while the lattice model displays a percolation behavior of the conductivity only for sufficiently large D/ξ values, which gradually crosses over to a tunneling-like regime as D/ξ decreases. For $D/\xi \lesssim 5$ we show that the conductivity of the lattice model is basically indistinguishable from that of the continuum case, establishing therefore a crossover point from percolation to tunneling behaviors.

This paper is organized as follows. In Sec. II we introduce the GTN model, we formulate the EMA for both lattice and continuum models and we calculate the resulting EMA conductances. In Sec. III we present our MC calculations for both the lattice and continuum models, and in Sec. IV we discuss the crossover between percolation and tunneling regimes. Discussions and conclusions are given in Sec. V

II. MODEL AND EFFECTIVE MEDIUM APPROXIMATION

The GTN model for conductor-insulator composites is defined by considering n identical conducting particles contained within a volume V . This defines the volume fraction $\phi = \rho v$ of the conducting phase, where $\rho = n/V$ is the particle density and v is the volume of a single particle. For the purpose of the present work we limit the analysis to the relatively simple case of spherical particles of identical diameter D , so that $v = \pi D^3/6$. Next, we assume that the tunneling conductance between any two particles centered at \mathbf{r}_i and \mathbf{r}_j is given by:

$$g(r_{ij}) = g_0 \exp\left[-\frac{2(r_{ij} - D)}{\xi}\right], \quad (1)$$

where g_0 is a constant ‘‘contact’’ conductance which in the following we shall set equal to unity, ξ is the characteristic tunneling length, and $r_{ij} = |\mathbf{r}_i - \mathbf{r}_j|$ is the distance between two sphere centers. For simplicity we further assume that selective tunneling mechanisms arising from excitation energies can be safely neglected (as in the case for nearest neighbor hopping⁶).

The set of all tunneling conductances of Eq. (1) defines a resistor network whose conductivity depends on ξ and D , as well as on the volume fraction ϕ and on the specific distribution of the particle centers. As shown below, it turns out that all these dependencies are well captured by the (single bond) EMA applied to the tunneling resistor network.² This is given by the solution of the following equation:

$$\left\langle \sum_{i \neq j} \frac{g(r_{ij}) - \bar{g}}{g(r_{ij}) + [Z_i Z_j / (Z_i + Z_j) - 1] \bar{g}} \right\rangle = 0, \quad (2)$$

where \bar{g} is the effective bond conductance and i and j run over the positions of the n particles. In the above expression, the symbol $\langle \dots \rangle$ denotes the statistical average over all realizations of the n -particle system. Furthermore, Z_i and Z_j are the coordination numbers of the two ends of a resistor $g(r_{ij})$, *i.e.*, given a particle at i (j), Z_i (Z_j) is the number of particles that are electrically connected to i (j). Since it is assumed that all particles are connected to each other regardless of their relative distances, $Z_i = Z_j = n - 1$. In this way, Eq. (2) reduces to

$$\left\langle \sum_{i \neq j} \frac{g(r_{ij}) - \bar{g}}{g(r_{ij}) + [(n-1)/2 - 1] \bar{g}} \right\rangle = 0. \quad (3)$$

By noticing that $\sum_{i \neq j} = n(n-1)$ and by using Eq. (1), we can write Eq. (3) more conveniently as

$$\left\langle \frac{1}{n} \sum_{i \neq j} \frac{1}{g^* \exp[2(r_{ij} - D)/\xi] + 1} \right\rangle = 2, \quad (4)$$

where for large n the dimensionless conductance $g^* = [(n-1)/2 - 1] \bar{g}/g_0 \simeq n \bar{g}/2g_0$ coincides with the conductance between two random nodes of the network with all bond conductances equal to \bar{g}/g_0 .¹⁰

By multiplying each term of the summation over i, j by $\int d\mathbf{r} \delta(\mathbf{r} - \mathbf{r}_{ij}) = 1$, where the integration is extended over the entire volume V , the left-hand side of Eq. (4) becomes

$$\begin{aligned} & \left\langle \frac{1}{n} \sum_{i \neq j} \int d\mathbf{r} \delta(\mathbf{r} - \mathbf{r}_{ij}) \frac{1}{g^* \exp[2(r_{ij} - D)/\xi] + 1} \right\rangle \\ &= \int d\mathbf{r} \left\langle \frac{1}{n} \sum_{i \neq j} \delta(\mathbf{r} - \mathbf{r}_{ij}) \right\rangle \frac{1}{g^* \exp[2(r - D)/\xi] + 1}. \end{aligned} \quad (5)$$

The above expression can be rewritten in terms of the pair distribution function $g_2(\mathbf{r})$ by noticing that, by definition:¹¹

$$\rho g_2(\mathbf{r}) = \left\langle \frac{1}{n} \sum_{i \neq j} \delta(\mathbf{r} - \mathbf{r}_{ij}) \right\rangle, \quad (6)$$

so that Eq. (4) reduces to

$$\int_0^\infty dr \frac{4\pi r^2 \rho g_2(r)}{g^* \exp[2(r - D)/\xi] + 1} = 2, \quad (7)$$

where $g_2(r) = \int d\Omega g_2(\mathbf{r})/4\pi$ is the radial distribution function (rdf) and the upper limit of the integration has been set to infinity because of the exponential decay of the integrand. Note that Eq. 7 is similar to the result obtained in Ref. 12.

An alternative and useful version of Eq. (7) can be obtained by introducing the function

$$W(r) = \frac{1}{g^* \exp[2(r - D)/\xi] + 1} = \frac{1}{\exp[2(r - r^*)/\xi] + 1}, \quad (8)$$

with

$$r^* = D + \frac{\xi}{2} \ln\left(\frac{1}{g^*}\right) \quad (9)$$

and integrating Eq. (7) by parts:

$$\int_0^\infty dr Z(r) \left(-\frac{dW(r)}{dr}\right) = 2, \quad (10)$$

where

$$Z(r) = \int_0^r dr' 4\pi r'^2 \rho g_2(r'), \quad (11)$$

is the cumulative coordination number function (*i.e.*, the number of spheres whose centers are within a distance r from the center of a given sphere).

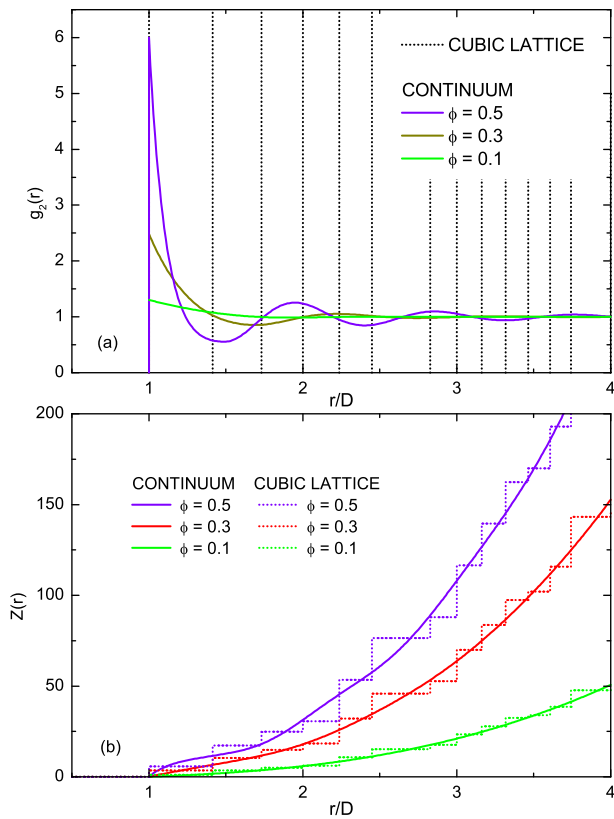


FIG. 1: (Color online) (a) Radial distribution function $g_2(r)$ for the lattice (dotted lines) and the continuum (solid lines) models. For the lattice model the vertical dotted lines indicate the positions of the delta-peaks centered at R_k for $k = 1, 2, 3, \dots$. The $g_2(r)$ curves for different ϕ values of the continuum model have been obtained by using the results of Ref. 14. (b) Cumulative coordination number $Z(r)$, Eq. (11), for the lattice (dotted lines) and the continuum (solid lines) models for different ϕ values.

A. Lattice and continuum models

As it is clear from the EMA equations (7) and (10), all the informations on the spatial distribution of the conducting particles is contained in the rdf $g_2(r)$, whose dependencies on r and ρ govern the behavior of the EMA conductance g^* . Here, we consider two possible realizations of a conductor-insulator composite which corresponds to two rather extreme forms of $g_2(r)$.

In the first case, we consider a simple cubic lattice with a lattice constant equal to the sphere diameter D , where only a fraction p of the lattice sites is occupied, randomly, by the spherical conducting particles, while the remaining fraction $1 - p$ is occupied by insulating spheres of equal diameter (as in the Scher and Zallen model of Ref. 13). The i -th conducting particle occupies therefore the position $\mathbf{r}_i = \mathbf{R}$ with probability $p = n/N$, where \mathbf{R} is the direct lattice vector running over all N sites of the cube. In this way, the pair distribution function defined

in Eq. (6) reduces to

$$\rho g_2(\mathbf{r}) = p \sum_{\mathbf{R} \neq \mathbf{0}} \delta(\mathbf{r} - \mathbf{R}), \quad (12)$$

which leads to an rdf of the form:

$$\rho g_2(r) = \frac{p}{4\pi} \sum_{k=1,2,\dots} \frac{N_k}{R_k^2} \delta(r - R_k), \quad (13)$$

where N_k is the number of the k -th nearest neighbors being at distance R_k from a reference particle set at the origin. The characteristic feature of this fractionally occupied lattice model is therefore that its rdf, shown in Fig. 1(a) by dotted lines, is given by delta-peaks whose positions do not change with p . As we shall see in the following, this feature is directly related to the appearance of a percolation behavior of the EMA conductance g^* for large D/ξ values.

The second model of particle distribution is given by an equilibrated dispersion of impenetrable spheres in the continuum. Typical examples of the resulting $g_2(r)$ for this case, obtained by using the formula provided in Ref. 14, are shown in Fig. 1(a) by solid lines and for different values of the volume fraction ϕ . As opposed to the lattice case, the rdf of an equilibrated dispersion of hard spheres is continuous and nonzero in the whole $r \geq D$ range, which we anticipate here to be the pre-requisite for an hopping behavior of the composite conductivity.

In Fig. 1(b) we compare the coordination number function $Z(r)$, Eq. (11), for the lattice (dotted lines) and continuum (solid lines) models. Contrary to the continuum model in which $Z(r)$ increases smoothly with r , the lattice $Z(r)$ has a step-like increase. At large r however the main contribution of the lattice $Z(r)$ goes as $(4/3)\pi\rho r^3$, meaning that the distribution of spheres in a sparsely occupied lattice is basically that of point particles in the continuum.

B. EMA conductance

Let us start by considering the solution of the EMA equation for the fractionally occupied cubic lattice case. By using Eq. (13) we find that Eq. (7) reduces to:

$$p \sum_{k=1,2,\dots} \frac{N_k}{g^* \exp[2(R_k - D)/\xi] + 1} = 2. \quad (14)$$

In the limiting case of very large particle sizes such that $D/\xi \rightarrow \infty$, only the first ($k = 1$) nearest neighbors with $R_1 = D$ and $N_1 = 6$ contribute to the summation in Eq. (14), which reduces to $6p/(g^* + 1) = 2$. Hence, in this limit, the resulting conductivity $g^* = 3(p - 1/3)$ has a percolation behavior and vanishes at the critical fraction $p_1 = 1/3$. For finite D/ξ values, the next nearest neighbors also contribute to the network conductivity. For example, by assuming that D/ξ is large enough to

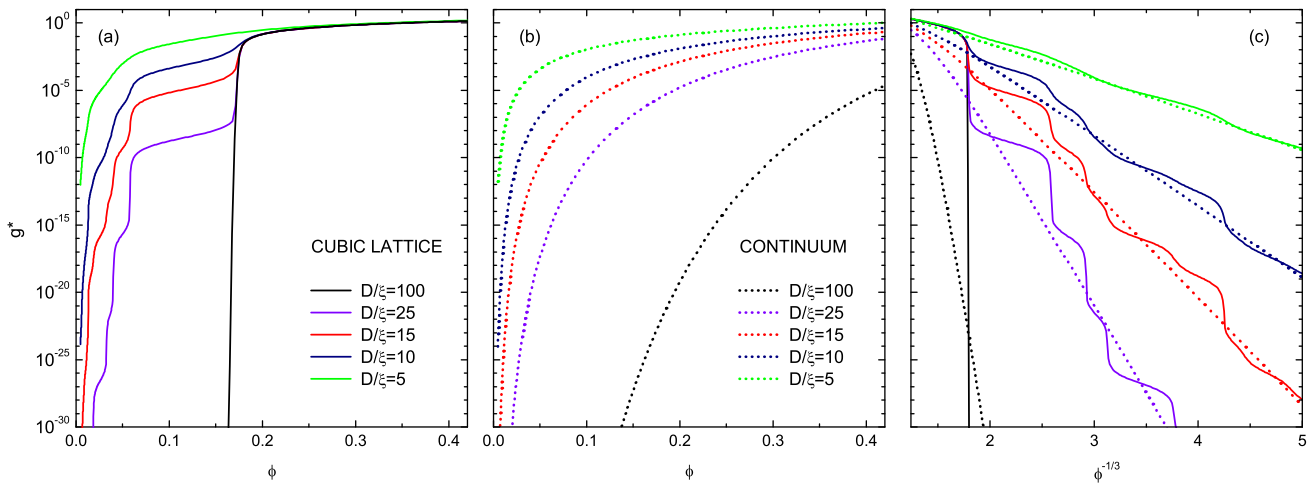


FIG. 2: (Color online) EMA conductance g^* for (a) the cubic lattice model and (b) the continuum model for different values of D/ξ . (c) EMA conductance of (a) and (b) plotted as a function of $\phi^{-1/3}$.

retain only the terms up to the second nearest neighbors ($N_2 = 12$ and $R_2 = \sqrt{2}D$) we get that Eq. (14) becomes

$$\frac{6p}{g^* + 1} + \frac{12p}{g^* \exp[2D(\sqrt{2} - 1)/\xi] + 1} = 2, \quad (15)$$

whose solution still behaves as $g^* \simeq p - p_1$ for $p > p_1$ but remains finite, albeit exponentially small, at lower p values. This is because the tunneling to the 2-nd nearest neighbors vanishes only at $p = p_2 = 1/9$. Considering the whole set of neighbors when p decreases, one finds that the solution of Eq. (14) becomes characterized by a monotonous decrease of g^* punctuated by sharp (for small D/ξ values) drops at $p = p_k$ with $p_k = 2/(\sum_{k'=1}^k N_{k'})$. Furthermore, in the vicinity of each p_k , the conductance follows the EMA power law behavior $\simeq (p - p_k)$ for $p > p_k$.

This feature is illustrated in Fig. 2(a) where we show numerical solutions of Eq. (14) for different values of D/ξ . For $D/\xi = 100$, the first percolation transition at $p_1 = 1/3$ ($\phi_1 = p_1\pi/6 \simeq 0.175$) causes a drop of the conductivity of about 36 orders of magnitude (not shown in the figure) compared to the conductivity at the close packing fraction $\pi/6$ that corresponds to the lattice sites that are all occupied by the conducting spheres. Such drop of the conductivity is well beyond the maximum range of conductivity values measured in real composites,¹⁵ and so, for all practical purposes, the $D/\xi = 100$ case behaves as $(\phi - \phi_1)^t$ with $t = 1$ being the EMA critical exponent. For $D/\xi = 25$ the first transition at ϕ_1 leads to a drop of g^* of only 8 orders of magnitude, and the transitions at lower values of ϕ are clearly visible in the figure. For lower values of D/ξ , the drops of g^* are further reduced and the transitions are much smoother, due of course to the fact that for these D/ξ values the probability of tunneling to neighbors that are farther apart is enhanced. For $D/\xi = 5$ the variation of

g^* is so smooth in the whole range of ϕ that the underlying lattice structure can be considered as completely irrelevant.

In contrast with the lattice case, the EMA conductance g^* resulting from an equilibrium distribution of conducting spheres in the continuum does not display any percolation behavior even for large D/ξ values. This is shown in Fig. 2(b) where solutions of Eq. (7), with $g_2(r)$ as given in Ref. 14, are plotted for the same D/ξ values of Fig. 1(a). The lack of percolation behavior in this case is due to the fact that the corresponding rdf [solid lines in Fig. 1(a)] is always nonzero for $r \geq D$ and it does not vary much even for ϕ values close to the packing fraction of the simple cubic lattice ($\phi = \pi/6 \simeq 0.524$). To see how the corresponding tunneling behavior arises, let us consider the EMA in the form of Eq. (10). Since, as shown in Fig. 1(b), the coordination number function $Z(r)$ is a smooth increasing function of r/D and, given that $-dW/dr$ is peaked at $r = r^*$ with spread $\simeq \xi$,¹⁶ we can approximate Eq. (10) by

$$Z(r^*) = 2, \quad (16)$$

so that, by applying Eq. (9), the EMA conductance becomes

$$g^* = \exp \left[-\frac{2(r^* - D)}{\xi} \right] \quad (17)$$

where r^* is such that Eq. (16) is satisfied. In passing, we note that Eqs. (16) and (17) represent the EMA equivalent of the critical path approximation (CPA) of Refs. 8,9.¹⁷ For sufficiently large r^* (*i.e.*, small g^*) the coordination number goes as $Z(r^*) \simeq (4/3)\pi\rho(r^*)^3$ and from Eq. (17) we obtain that

$$g^* \simeq \exp \left[-\frac{2D}{\xi} \left(\frac{0.63}{\phi^{1/3}} - 1 \right) \right], \quad (18)$$

which coincides, if the coefficient 0.63 in the exponent is replaced by 0.7, with the low-density hopping behavior as obtained from the CPA.⁸ In the same low-density limit, Eq. (18) (with a slightly different coefficient in the exponent) has been derived also in Ref. 12 by using an EMA-based procedure similar to the one presented here.

The hopping-like (or tunneling-like) dependence of g^* for the continuum model is further illustrated in Fig. 2(c) where the results of Fig. 2(b) have been re-plotted as a function of $\phi^{-1/3}$ (dotted lines). In Fig. 2(c) we show for comparison also the g^* versus $\phi^{-1/3}$ curves (solid lines) of the lattice model results of Fig. 2(a), which tend, with the decrease of D/ξ , to the tunneling behavior of the continuum model. An asymptotic equivalence between the two models is indeed expected because, as noted above, the underlying microstructures become irrelevant for small D/ξ . Mathematically, this can be seen from Eq. (10) since $-dW/dr$ averages $Z(r)$ within a distance $\simeq \xi$ around r^* , and thus the differences between the lattice and the continuum models are blurred for sufficiently large ξ . Note also that for the lattice model $Z(r^*) \simeq (4/3)\pi\rho(r^*)^3$ for large r^* , implying that g^* tends asymptotically to the results given by Eq. (18), as shown by the solid lines in Fig. 2(c).

III. MONTE CARLO RESULTS

Let us turn now to a comparison of our EMA results of the previous section with full MC calculations of the conductivity for both the lattice and continuum models. For the continuum we have generated equilibrium distributions of impenetrable spheres inside a cubic cell with periodic boundary conditions following the procedure that we outlined previously in Refs. 4,5. For the lattice model, we simply populated a given fraction of the cubic lattice sites with conducting spheres with diameter equal to the cubic lattice constant.

To calculate the conductivity resulting from the lattice and continuum models, we ascribed to each pair of particles the tunneling conductance of Eq. (1), and performed a numerical decimation of the resulting resistor network.^{4,5,18} To reduce computational times of the decimation procedure we introduced an artificial maximum distance between the particles beyond which the resulting bond conductance can be safely neglected.^{4,5}

The results of the calculated conductivity are plotted in Fig. 3 for the same parameter values that were used for Fig. 2. Each symbol is the outcome of $N_R = 50$ realizations of systems of $N_P \sim 1000$ spheres. The logarithm average of the results was considered since, due to the exponential dependence of Eq. (1), the distribution of the computed conductivities was approximately of the log-normal form.

It is interesting to notice that there is an overall quasi-quantitative agreement between the EMA and the MC results, for both lattice and continuum models, meaning that the EMA formulation of Sec. II captures well

the physics of the problem. For example, the first percolation threshold at $p_1 = 1/3$ ($\phi_1 = \pi p_1/6 \simeq 0.175$) obtained from the EMA on the cubic lattice is very close to the critical value $p_1 \simeq 0.3116$ ($\phi_1 \simeq 0.163$) for the site percolation problem on the simple cubic lattice.^{1,2,19} An important expected difference is however found in the region $\phi > \phi_1$ where the MC conductivity for the lattice case should follow a $(\phi - \phi_1)^t$ dependence with a critical exponent $t \simeq 2$ instead of the EMA exponent of $t = 1$.² This is indeed verified in Fig. 4 where the MC conductivities for $D/\xi = 25$ (a) and $D/\xi = 15$ (b) are both fitted with $t \simeq 1.56 \pm 0.04$, which is slightly lower than $t \simeq 2$ due to finite size effects (for the same reason we find $\phi_1 \simeq 0.18$ instead of $\phi_1 \simeq 0.163$). Similar critical behaviors are expected in the vicinity of all consecutive percolation thresholds ϕ_k with $k > 1$, but due to the limited number of particle densities considered in our MC calculations and the close proximity of successive p_k values we have been able to fit only the $D/\xi = 25$ case in the vicinity of the second percolation threshold. We have found $t = 1.76 \pm 0.15$, which agrees within errors with the exponent at ϕ_1 , and $\phi_2 \simeq 0.074$ ($p_2 \simeq 0.141$) which is close to the expected value $\phi_2 \simeq 0.072$ ($p_2 \simeq 0.137$).²⁰ These same values of t and ϕ_2 appear to reproduce quite well the percolation behavior around the second percolation threshold also for the $D/\xi = 15$ case [Fig. 4(b)].

Another important agreement between the EMA and the MC results is the tendency of the lattice model conductivity to become tunneling-like as D/ξ decreases. This is illustrated in Fig. 3(c) where the MC conductivities of Fig. 3(a) and Fig. 3(b) are plotted as functions of $\phi^{-1/3}$. The asymptotic regime for small σ of the continuum model (open symbols) follow Eq. (18) with the coefficient 0.63 replaced by 0.7, as obtained from the critical path approximation applied to a dilute system of impenetrable spheres.⁸ In complete analogy with the EMA results, the conductivities of the lattice model [filled symbols in Fig. 3(c)] steadily tend to this tunneling regime as D/ξ decreases, and for $D/\xi = 5$ the MC results of the two models are practically indistinguishable for all values of ϕ .

IV. PERCOLATION-TO-HOPPING CROSSOVER

Both EMA and MC results point toward a substantial equivalence between the cubic lattice and the continuum models for sufficiently small values of D/ξ . Given that the two models considered represent two extreme limits of how the conducting particles may be ideally arranged in an insulator-conductor composite, such equivalence is important for the understanding of the transport properties in real composites, whose microstructure is neither completely lattice-like nor exactly an equilibrium distribution in the continuum. We find it therefore useful to define a measure for the deviation between the lattice and continuum models in order to follow quantitatively

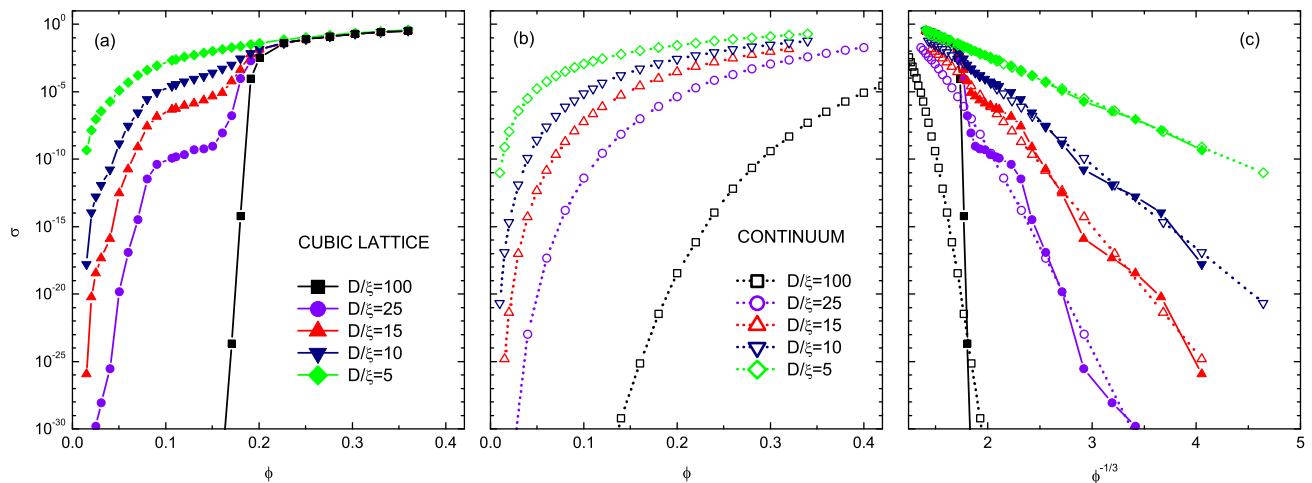


FIG. 3: (Color online) Monte Carlo conductance for (a) the cubic lattice model and (b) the continuum model for different values of D/ξ . (c) The same results of (a) and (b) plotted as a function of $\phi^{-1/3}$.

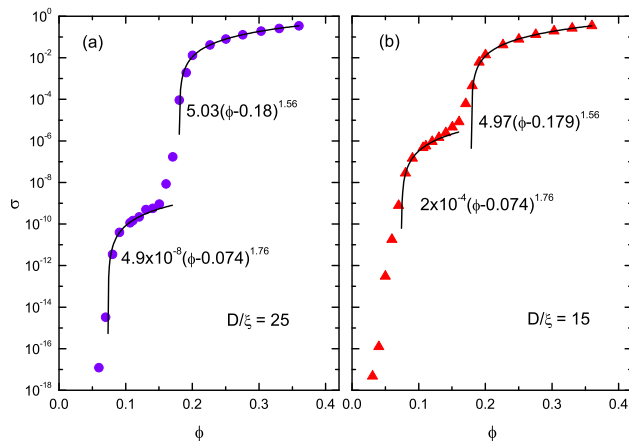


FIG. 4: (Color online) The lattice Monte Carlo conductivity as a function of ϕ for (a) $D/\xi = 25$ and (b) $D/\xi = 15$. The solid lines are the best fits with the percolation formula $\sigma = \sigma_0(\phi - \phi_c)^t$.

how these two extremes approach each other as D/ξ decreases.

To this end, we introduce the following quantity:

$$\Delta = \left| \log \left(\frac{\sigma_{\text{latt.}}}{\sigma_{\text{cont.}}} \right) \right|, \quad (19)$$

where $\sigma_{\text{latt.}}$ and $\sigma_{\text{cont.}}$ are the conductivities for the lattice and the continuum models, respectively, and the log is the logarithm with base 10. Hence, according to Eq. (19), $\Delta = M$ if for a certain ϕ value $\sigma_{\text{latt.}}$ differs from $\sigma_{\text{cont.}}$ by M orders of magnitude. In Fig. 5 we plot the maximum value Δ_{max} and the mean value Δ_{mean} of Δ as calculated over the entire range of ϕ considered and for several values of D/ξ . The open symbols are the Δ_{max} and Δ_{mean} values as extracted from the EMA

calculations while the filled symbols refer to the MC results. As clearly seen in the figure, when D/ξ decreases both Δ_{max} and Δ_{mean} . For $D/\xi < 10$, Δ_{max} becomes less than unity, which means that $\sigma_{\text{latt.}}$ and $\sigma_{\text{cont.}}$ differ at most by less than one order of magnitude in the whole range of ϕ values. We also note that for $D/\xi < 10$ the MC results display a somewhat stronger decrease than the EMA results. This feature does not seem to be due to finite size effects in the MC calculations, and we attribute it to a real deviation from the EMA results. We can then identify the value of $D/\xi \simeq 5$ as a crossover between percolation and hopping regimes below which the conductivities of the lattice and continuum models differ significantly less than one order of magnitude.

As repeatedly stressed above, the lattice and continuum models are rather idealized representations of the true microstructure of real conductor-insulator composites. However they also define two extreme boundaries which delimit somehow all the possible configurations that can be found in isotropic and homogeneous composites. For this reason, the results of Fig. 5 can be considered as upper boundaries of more realistic composites, and our $D/\xi \simeq 5$ result probably underestimates the crossover point between percolation and hopping for composites whose microstructure deviates from an ideal lattice model.

V. DISCUSSION AND CONCLUSIONS

The results presented in the previous sections consistently show that the GTN model of conductor-insulator composites, where each particle is connected via tunneling to all others, is capable of explaining the appearance of both percolation and hopping regimes depend-

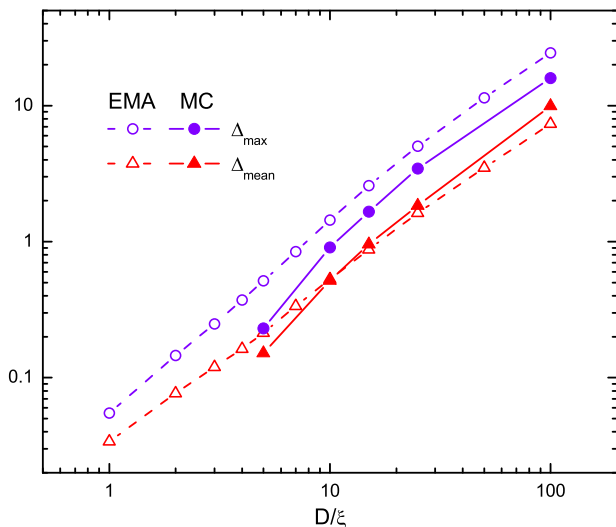


FIG. 5: (Color online) Maximum value Δ_{\max} and mean value Δ_{mean} extracted from the whole ϕ dependence of Eq. (19) and for several values of D/ξ . The open symbols are the EMA results, while the filled symbols refer to the MC calculations.

ing on few characteristics of the composite. In particular, we have identified the ratio D/ξ and the composite microstructure as the relevant variables that control the switch from one regime to the other. For large values of D/ξ , percolation arises in composites whose microstructure can approach a regular lattice that is fractionally occupied by conducting particle, while a hopping regime of the conductivity is always obtained for equilibrium distributions of conducting particles in the continuum. As D/ξ decreases, the conductivity of the lattice-like composites gradually loses its percolating character and approaches the hopping regime which characterizes the continuum limit. For $D/\xi \lesssim 5$ the composite conductivity displays hopping behavior independent of the specific microstructure and is practically indistinguishable from that arising from an equilibrium distribution of particles in the continuum.

Given that the values of the tunneling characteristic length ξ do not exceed a few nanometers, our analysis predicts that composites whose conducting fillers have nanometric sizes should always display a hopping-like (*i. e.*, percolation-less) behavior independent of the particular distribution of the conducting particles in the composite. Instead, composites with conducting filler sizes larger than a fraction of microns should display percolation or hopping behaviors depending on the whether the microstructure is more lattice-like or more continuum-like, respectively. In view of the above, it appears then reasonable that dilute filler polymer-based composites will display hopping-like behavior also for filler diameters substantially larger than ξ (*i. e.*, in the order of some hundreds of nanometers) as we have verified recently in Ref. 5. At the same time, our theory also explains the conductivity behavior of composites made of mixtures of

hard conducting and insulating particles. In particular, we note that in dense ensembles of conducting spheres the arrangement in continuum systems is similar to that of lattices.^{13,21,22} In this respect, the results of Ref. 23 on the conductivity of co-sputtered Ni-SiO₂ cermets represent a nice example of tunneling-driven percolating behavior on a lattice-like microstructure. Indeed, the data of Ref. 23 display multiple percolation thresholds as the concentration of conducting Ni grains is reduced, very much like the behavior shown in Fig. 4 for the MC conductivity of a fractionally occupied lattice model. The difference of about 3 orders of magnitude between the conductivity at the largest Ni concentration and that at the first percolation threshold can be reproduced by our model by setting $D/\xi \simeq 10$ which, by using the measured mean Ni grain size $D \approx 10$ nm,²³ leads to $\xi \approx 1$ nm, which is of the expected order of magnitude (see e.g. Refs. 6,8) and compares well with the ξ values extracted from other composites with spherical fillers.^{4,5} It should be noted however that the lattice model applies only partially to the Ni-SiO₂ data because the nonuniversal value of the conductivity exponent t observed in the vicinity of the second percolation threshold in Ref. 23 cannot be reproduced by our lattice MC results (see Fig. 4). As to be discussed elsewhere, a nonuniversal value of t (in the sense that we have specified in Refs. 18,24) could be obtained within the GTN model by allowing a finite dispersion in the distances of the second nearest neighbors.

Before concluding it is worth to point out some limitations of the theory presented above. First, for simplicity, we have considered composites whose conducting fillers are given by monodispersed spheres. Even maintaining that for some classes of composites the shape of the fillers can be approximated by a sphere, the collection of such spheres in a real composite has however some degree of polydispersivity, which can be large enough to make the fractionally occupied periodic lattice model an inappropriate description of the possible configuration of the microstructure. However, as stressed above, the lattice model should be regarded as an extreme deviation from a continuum dispersion of particles (monodispersed or not), so that the crossover studied in Sec. IV represents an upper limit also for the case of polydispersed spherical particles. The second limitation is associated with the fact that we have limited ourselves to the case of isotropic particle fillers, and we have not attempted to analyze how percolation and hopping behaviors arise for anisotropic filler shapes such as rodlike or platelike particles. An analysis of these cases would be interesting also in relation to the appearance of nematic phases for large volume fractions of anisotropic fillers and to lattice-like arrangements driven by attractive forces in dispersions of rodlike particles.

Acknowledgments

This work was supported in part by the Israel Science Foundation (ISF), and in part by the Swiss National Sci-

ence Foundation (Grant No. 200021-121740).

-
- * Electronic address: gianluca.ambrosetti@a3.epfl.ch
 † Electronic address: claudio.grimaldi@epfl.ch
- ¹ D. Stauffer and A. Aharony, *Introduction to Percolation Theory* (Taylor & Francis, London 1994).
 - ² M. Sahimi, *Heterogeneous Materials I. Linear Transport and Optical Properties* (Springer, New York, 2003).
 - ³ I. Balberg, J. Phys. D: Appl. Phys. **42**, 064003 (2009).
 - ⁴ G. Ambrosetti, N. Johnner, C. Grimaldi, T. Maeder, P. Ryser, and A. Danani, J. Appl. Phys **106**, 016103 (2009).
 - ⁵ G. Ambrosetti, C. Grimaldi, I. Balberg, T. Maeder, A. Danani, and P. Ryser, Phys. Rev. B **81**, 155434 (2010).
 - ⁶ B. I. Shklovskii and A. L. Efros, *Electronic Properties of Doped Semiconductors* (Springer, Berlin, 1984).
 - ⁷ V. Ambegaokar, B. I. Halperin, and J. S. Langer, Phys. Rev. B **4**, 2612 (1971); M. Pollak, J. Non Cryst. Solids **11**, 1 (1972); B. I. Shklovskii and A. L. Efros, Sov. Phys. JETP **33**, 468 (1971); **34**, 1084 (1972).
 - ⁸ C. H. Seager and G. E. Pike, Phys. Rev. B **10**, 1435 (1974).
 - ⁹ H. Overhof and P. Thomas, *Hydrogenated Amorphous Semiconductors* (Springer, Berlin, 1989).
 - ¹⁰ E. López, S. Carmi, S. Havlin, S. V. Buldyrev, and H. E. Stanley, Physica D **224**, 69 (2006).
 - ¹¹ J. -P. Hansen and I. R. McDonald, *Theory of Simple Liquids* (Elsevier, 2006).
 - ¹² B. Movaghar and W. Schirmacher, J. Phys. C **14**, 859 (1981).
 - ¹³ H. Scher and R. Zallen, J. Chem. Phys. **53** 3759 (1970).
 - ¹⁴ A. Trokhymchuk, I. Nezbeda, J. Jirsák, and D. Henderson, J. Chem. Phys. **123**, 024501 (2005); Erratum, J. Chem. Phys. **124**, 149902 (2006).
 - ¹⁵ As discussed in Ref. 5, the lowest measurable conductivity is limited either by the experimental apparatus or by the intrinsic conductivity of the insulating phase.
 - ¹⁶ Note that, since the function $W(r)$ in Eq. (8) has the form of a Fermi distribution with $\xi/2$ playing the role of temperature, one has $-dW/dr \rightarrow \delta(r - r^*)$ for $\xi \rightarrow 0$.
 - ¹⁷ We remind that the CPA amounts to keep only the subset of tunnel conductances $g(r_{ij})$ having $r_{ij} \leq r_c$, where r_c is the largest among the inter-particle distances such that the so-defined subnetwork forms a conducting percolating cluster. It then follows that r_c is such that $Z(r_c) = Z_c$ is satisfied, where Z_c is the critical coordination number. Finally the CPA is obtained by assigning the value $g_c = g_0 \exp[-2(r_c - D)/\xi]$ to all the tunnel conductances of the entire network. In the present EMA version of the CPA, g_c is replaced by g^* , Eq. (17), and the criterion $Z(r_c) = Z_c$ is replaced by Eq. (16).
 - ¹⁸ N. Johnner, C. Grimaldi, I. Balberg and P. Ryser, Phys. Rev. B **77**, 174204 (2008).
 - ¹⁹ Y. J. Deng and H. W. J. Blote, Phys. Rev. E **72**, 016126 (2005).
 - ²⁰ G. E. Pike and C. H. Seager, Phys. Rev. B **10**, 1421 (1974).
 - ²¹ N. L. Lavrik and V. P. Voloshin, J. Chem. Phys. **114** 9489 (2001).
 - ²² V. S. Kumar and V. Kumaran, J. Chem. Phys. **123** 074502 (2005).
 - ²³ D. Toker, D. Azulay, N. Shimoni, I. Balberg, and O. Millo Phys. Rev. B **68**, 041403(R) (2003).
 - ²⁴ C. Grimaldi and I. Balberg, Phys. Rev. Lett. **96**, 066602 (2006).